(23) R. Deslauriers, I. C. P. Smith, and R. Walter, *J. Biol. Chem.*, **249**, 7006 (1974).
(24) F. A. Bovey in "Chemistry and Biology of Peptides", J. Meinenhofer, Ed., Ann Arbor Science Publishers, Ann Arbor, Mich., 1972, pp 3–28.
(25) I. C. P. Smith, R. Deslauriers, and R. Walter in "Chemistry and Biology of Peptides", J. Meienhofer, Ed., Ann Arbor Science Publishers, Ann Arbor, Mich., 1972, pp 29–34.
(26) M. Rothe, K. D. Steffen, and I. Rother, *Angew. Chem., Int. Ed. Engl.*, **4**, 356 (1965).
(27) A. C. T. North, D. C. Phillips, and F. S. Mathews, *Acta Crystallogr., Sect. A*, **24**, 351 (1968).
(28) C. L. Coulter, *J. Am. Chem. Soc.*, **95**, 570 (1973).
(29) C. L. Coulter and N. R. Cozzarelli, *J. Mol. Biol.*, **91**, 329 (1975).
(30) D. Cremer and J. A. Pople, *J. Am. Chem. Soc.*, **97**, 3244 (1975).
(31) "International Tables for X-Ray Crystallography", Vol. IV, Kynoch Press, Birmingham, England, 1974.
(32) R. E. Marsh and J. Donohue, *Adv. Prot. Chem.*, **22**, 235 (1967).
(33) T. Ashida and M. Kakudo, *Bull. Chem. Soc. Jpn.*, **47**, 1129 (1974).
(34) J. Donohue in "Structural Chemistry and Molecular Biology", A. Rich and N. Davidson, Ed., W. H. Freeman, San Francisco, Calif., 1968, pp 443–465.
(35) C. M. Venkatachalam, *Biochim. Biophys. Acta*, **168**, 397 (1968).
(36) D. Lavallee, unpublished, 1973.
(37) R. Deslauriers, M. Rothe, and I. C. P. Smith, ref 14, pp 91–96.
(38) R. Somorjai and R. Deslauriers, in preparation, 1976.
(39) J. E. Kilpatrick, K. S. Pitzer, and R. Spitzer, *J. Am. Chem. Soc.*, **69**, 2483 (1947).
(40) K. S. Pitzer and W. E. Donath, *J. Am. Chem. soc.*, **81**, 3213 (1959).

Kinetics and Mechanism of Molybdate and Tungstate Complex Formation with Catechol Derivatives[1]

Katharine Gilbert and Kenneth Kustin*

Contribution from the Department of Chemistry, Brandeis University, Waltham, Massachusetts 02154. *Received September 22, 1975*

Abstract: Rate constants for the complexation of molybdate and tungstate with catechol derivatives have been determined at 25 ± 1 °C and ionic strength 0.5 M (NH_4Cl) by the approach-to-equilibrium technique on a stopped-flow apparatus. Ligands studied were 1,2,4- and 1,2,3-trihydroxybenzene (pyrogallol), 3,4,5-trihydroxybenzoic acid (gallic acid), 3,4-dihydroxyphenylalanine (L-Dopa), and [3,4-dihydroxyphenyl]-2-methylaminoethanol (D-epinephrine). The formation of the mono (1:1) complex is more rapid for protonated than for unprotonated oxyanion. From the hydrogen ion dependence of the relaxation time it was determined that reactions of completely deprotonated ligand with completely deprotonated oxyanion, and completely protonated ligand with protonated oxyanion, do not contribute, within experimental error, to the observed rate of complexation. The relaxation times (standard deviations ±5%, except for pyrogallol and 1,2,4-trihydroxybenzene ±10%) consist of acid-independent and -dependent parts which contain kinetically indistinguishable terms for which upper limits could be deduced by setting all but one term equal to zero. Some of the upper limits exceed diffusion control allowing minimum limits to be set for the terms previously set equal to zero. For some pathways the upper and lower limits are approximately the same, leading to the actual value within experimental error and the uncertainties in the associated acid dissociation constants and estimated diffusion controlled rate constants. For molybdate and tungstate complexations with these and other ligands a trend in complex formation rate constant with basicity occurs. Namely, if the oxyanion is protonated the most basic ligand is most reactive. If the oxyanion is unprotonated, the least basic ligand is most reactive. The fastest rate of complex formation occurs when the protonated oxyanion reacts with the most basic ligand fully deprotonated at the binding sites. These trends are explained by assuming that the tetrahedral unprotonated oxyanion reacts by an addition mechanism, and the (postulated) octahedral protonated oxyanion reacts by a substitution mechanism. Ligand basicity then controls complex formation in substitution by assisting elimination of the OH^- groups to be replaced through a hydrogen-bond-transfer mechanism, but hinders addition through the same effect. For 1,2,4-trihydroxybenzene the kinetics of formation of mono and bis complexes has been determined at ionic strength 0.1 M. Unlike the formation of the mono complex, the formation rate of the bis complex decreases with decreasing pH. This effect is also explained by the fact that the reactive metal-containing species in the higher order complex formation step is already octahedrally coordinated. There is no conversion to octahedral form upon protonation, and the influence of ligand protonation dominates the process.

Metal-containing oxyanions readily form complexes with numerous different types of nucleophilic reagents.[2] In this regard, they resemble simple, aquated di- and trivalent metal ions. For the aquated metal ions, the mechanism of complexation is well understood, being based on one essential feature. Complex formation is a substitution process, controlled by the breaking of the metal–water bond in the formation of a reduced coordination-number activated complex.[3] Exceptions to this mechanism are few, and do not show wide variations in ligand substitution rate constants.[4] We now have several thorough kinetics studies of oxyanion–ligand systems: chromate,[5-7] vanadate,[8] molybdate,[9-12] and tungstate,[10,13] for example. It is thus appropriate to determine the context in which to view the mechanism of these reactions.

One ambiguity immediately presents itself, however, making it difficult to achieve a mechanistic synthesis similar to that for the simple aquated metal ions. The structures in solution of monomeric oxyanions are not clear. The unprotonated species (MoO_4^{2-}, WO_4^{2-}, etc.) are probably tetrahedral;[14] yet, addition of a proton to MoO_4^{2-} is not diffusion controlled,[15] implying that a structural change, perhaps tetrahedral to octahedral coordination, accompanies the reaction. Certainly, the known solid-state structures of molybdate and tungstate oxyanion complexes are octahedral,[16] with cis-dioxygen coordination in the absence of full occupation by the complexing ligand or ligands. This situation has led some investigators to regard oxyanion complexation and oxyanion polymerization (or condensation) as examples of addition rather than substitution.[9,17] This point, though interesting, is less fundamental than determining the trends, if any, in the complex formation rate constants with variations in ligand properties.

Ligand discrimination by oxyanions has been discussed for CrO_4^{2-},[7] where it may be present, but is obscured by accompanying catalytic behavior, and for MoO_4^{2-} and WO_4^{2-} with substituted 8-hydroxyquinolines.[10] With these ligands, it was established that the main pathways for complexation involve the protonated oxyanion. No conclusion was drawn with respect to the influence of, say, ligand basicity on the rate of complex formation. In order to gain more information on the role played by ligand basicity in this type of reaction, a systematic investigation of the kinetics of complex formation with one ligand and several of its derivatives was undertaken.

As complexes between oxyanions and catechol and its derivatives have been well characterized,[18-20] and afford a reasonable range in basicity, we are reporting the results of a kinetics study with several of these compounds. A start had already been made in the case of catechol itself.[11] Catecholamines are frequently of potent physiological activity,[21] e.g., as hormones, but are not commonly regarded as ligands. These, and the other catechol chelating agents used, are named and shown below.

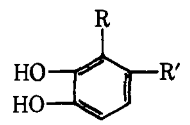

1,2-dihydroxybenzene: R = R′ = H; catechol
1,2,3-trihydroxybenzene: R = OH, R′ = H; pyrogallol
1,2,4-trihydroxybenzene: R = H, R′ = OH

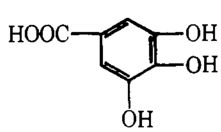

3,4,5-trihydroxybenzoic acid: gallic acid

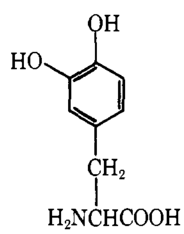

3,4-dihydroxyphenylalanine: L-Dopa

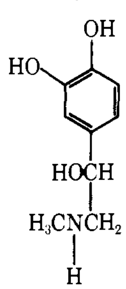

[3,4-dihydroxyphenyl]-2-methylaminoethanol: L-epinephrine (adrenaline)

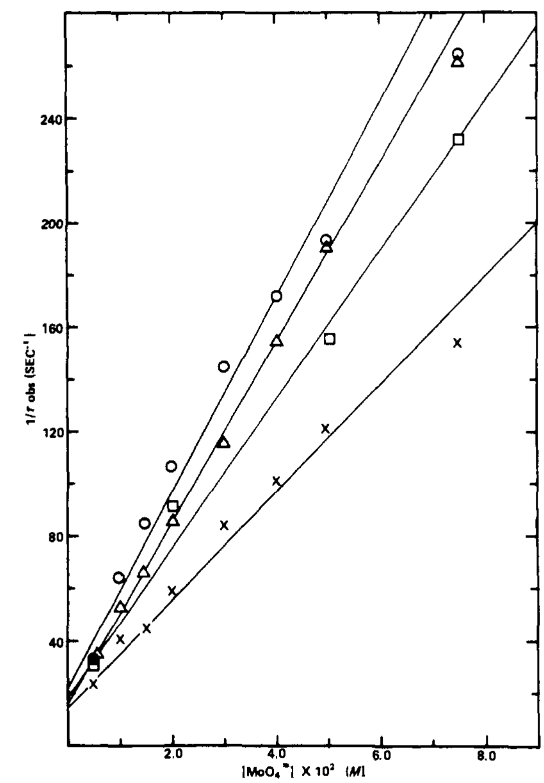

Figure 1. Plot of $1/\tau_{obsd}$ against molybdate concentration for the formation of the 1:1 complex between gallic acid and molybdate. Total initial gallic acid concentration = 1.9×10^{-4} M, T = 25 °C, ionic strength = 0.5 M; ○ = pH 7.3; △ = pH 7.7; □ = pH 8.0; × = pH 8.3. Calculated least-squares straight lines have been drawn through the data points. At the highest concentrations of oxyanion studied, the data points tend to fall below the calculated values, especially at the lowest pH's studied. This effect is due to the slight amount of molybdate polymerization occurring in these solutions.

Experimental Section

Materials. The following reagent grade chemicals were used without further purification: 1,2,4-trihydroxybenzene (Aldrich); ammonium hydroxide, pyrogallol, gallic acid, sodium tungstate (Baker); L-epinephrine (Calbiochem.); sodium bisulfite ($Na_2S_2O_5$), sodium molybdate (Fisher); ammonium chloride (Mallincrodt); and L-Dopa (Nutritional Biochemical Corp.). The ligand solutions were prepared fresh by weight for each experiment; the molybdate and tungstate were taken from 0.50 M stock solutions. Water was doubly distilled.

Kinetics Studies. All kinetics studies were run on a stopped-flow apparatus equipped with a Biomation 610B transient recorder and Datacap E103 coupler interfaced to a Teletype 33 ASR for direct digital output on paper tape.[22] Least-squares routines,[23] run on a PDP-10 computer, were then carried out to obtain relaxation times (as in the approach-to-equilibrium method), followed by overall forward and reverse rate constant determinations by weighted least squares.

The kinetics studies were carried out at 25 ± 1 °C and ionic strength 0.5 M (NH_4Cl), unless otherwise noted. In the 1:1 studies reaction rates were measured under pseudo-first-order conditions with the concentration of oxyanion ($0.25–7.50 \times 10^{-2}$ M) in large excess (>25-fold) over that of ligand ($1.00–3.00 \times 10^{-4}$ M). To avoid oxyanion condensation, molybdate solutions were all at pH ≥7.3 and those of tungstate at pH ≥8.0. Oxidation of the catechol derivatives was minimized by bubbling argon through the ligand solutions and adding sodium bisulfite (0.01 M). Control experiments without bisulfite showed that this reagent did not affect the relaxation times significantly.

After ammonium chloride was added to bring the solutions to 0.5 M ionic strength, the pH was adjusted and buffered with ammonium hydroxide. The hydrogen ion concentration was measured with Corning Model 7 and Radiometer pH meters. The experimental runs were monitored spectrophotometrically at 340 nm.

At a given pH and oxyanion concentration, we made at least five experimental determinations of the relaxation times. The standard deviations of the relaxation times were within ±5%, except for pyrogallol and 1,2,4-trihydroxybenzene, which were within ±10%.

To observe the rate of the second step of chelation to form a 1:2 = metal oxyanion:ligand complex, 1,2,4-trihydroxybenzene ($0.29–1.52 \times 10^{-2}$ M) was present in great excess (at least 200-fold) over the concentration of oxyanion (1.5×10^{-5} M). Ionic strength was 0.1 M (NH_4Cl) and all other conditions and methods were as previously described for the first step. Some studies of the first step of complexation of molybdate with 1,2,4-trihydroxybenzene were also carried out at ionic strength 0.1 M.

Results and Treatment of Data

Oxyanion Dependence. The observed pseudo-first-order relaxation times for the complexation of molybdate with catechol derivatives are shown in Table I; those for tungstate with catechol derivatives are shown in Table II. Because the concentrations of the metal were always in large excess over that of the ligand, close to equilibrium conditions obtain, and the

Table I. Observed Relaxation Times for the 1:1 Complexation of Molybdate with Catechol Derivatives

Ligand	$10^2[MoO_4^{2-}]$ (M)	$1/\tau_{obsd}$ (s^{-1}) pH											
		7.3	7.7	7.8	8.0	8.2	8.3	8.4	8.5	8.6	8.7	8.8	9.0
1,2,4-Trihydroxybenzene	0.75	16.8	—	—	—	—	—	—	—	—	—	—	—
	1.00	22.7	—	—	—	—	—	—	—	—	12.3	12.8	—
	1.50	31.0	—	26.2	—	22.4	—	—	—	—	14.1	14.4	13.4
	1.90	—	—	28.9	—	—	—	—	—	—	—	—	—
	2.00	30.8	—	32.3	—	26.3	—	—	—	—	14.8	15.9	14.4
	2.50	33.8	—	34.2	—	27.3	—	—	27.2	—	16.2	17.3	14.8
	2.90	38.4	—	—	—	—	—	—	—	—	—	—	—
	3.00	42.3	—	36.8	—	29.7	—	—	—	—	17.8	19.6	16.7
	3.50	—	—	—	—	34.3	—	—	—	—	—	—	—
	4.00	46.7	—	—	—	37.5	—	—	36.9	—	—	20.5	17.4
	4.50	—	—	—	—	—	—	—	—	—	—	—	19.1
	5.00	50.2	—	47.4	—	39.2	—	—	41.5	—	—	25.1	—
	5.50	—	—	—	—	—	—	—	42.2	—	—	—	22.6
	6.00	—	—	51.5	—	—	—	—	46.2	—	—	—	—
	6.50	—	—	—	—	—	—	—	49.0	—	—	—	23.6
	7.00	—	—	56.1	—	49.9	—	—	48.1	—	32.5	31.7	26.4
	7.50	—	—	—	—	51.2	—	—	50.9	—	—	—	—
10^4[Ligand]$_0$ (M)		2.1	—	2.1	—	2.1	—	—	2.1	—	—	—	—
Pyrogallol	0.50	—	29.1	—	29.2	—	—	—	—	—	—	—	—
	0.75	23.0	42.8	—	35.7	—	—	26.6	—	18.2	—	—	13.0
	1.00	23.2	48.8	—	47.5	—	—	—	—	17.1	—	—	10.6
	1.50	27.9	67.7	—	68.0	—	—	—	—	24.0	—	—	12.3
	2.00	37.2	71.2	—	80.9	—	—	—	—	28.4	—	—	13.9
	2.50	—	91.2	—	81.6	—	—	46.1	—	—	—	—	—
	3.00	45.6	91.7	—	93.2	—	—	51.7	—	37.4	—	—	15.7
	3.75	54.3	—	—	115.	—	—	110.	—	45.8	—	—	23.4
	4.00	—	132.	—	112.	—	—	—	—	47.2	—	—	17.5
	5.00	68.5	—	—	155.	—	—	92.3	—	52.9	—	—	20.25
	6.00	74.5	—	—	195.	—	—	145.	—	53.8	—	—	28.6
	7.00	—	—	—	—	—	—	130.	—	—	—	—	—
	7.50	84.5	—	—	—	—	—	161.	—	61.4	—	—	26.0
10^4[Ligand]$_0$ (M)		1.0	1.0	—	1.0	—	—	1.0	—	1.0	—	—	1.0
Gallic acid	0.50	33.8	34.4	—	32.7	—	23.5						
	1.00	63.2	53.0	—	—	—	41.6						
	1.50	85.3	66.0	—	—	—	45.1						
	2.00	106.	86.3	—	90.1	—	59.2						
	3.00	145.	115.	—	—	—	84.7						
	4.00	173.	155.	—	—	—	100.8						
	5.00	194.	191.	—	155.	—	120.						
	7.50	264.	262.	—	232.	—	154.						
10^4[Ligand]$_0$ (M)		2.9	1.9	—	1.9	—	1.6						
Epinephrine	0.50	9.62	10.05	—	9.82	—	9.43						
	1.00	—	14.5	—	13.5	—	—						
	1.50	—	16.7	—	—	—	—						
	2.00	22.0	20.6	—	21.4	—	19.4						
	3.00	—	28.0	—	27.6	—	—						
	4.00	—	36.0	—	33.5	—	—						
	5.00	42.6	42.0	—	44.7	—	37.3						
	6.00	—	—	—	—	—	—						
	7.50	56.6	52.4	—	51.4	—	49.8						
10^4[Ligand]$_0$ (M)		1.5	1.7	—	1.4	—	2.0						
L-Dopa	0.50	—			9.59				7.79			7.63	4.81
	1.00	11.4			12.2				11.3			10.5	—
	1.50	18.9			—				14.5			13.9	8.18
	2.00	21.9			—				17.8			18.2	9.99
	2.50	—			21.8				—			—	—
	3.00	28.4			—				23.4			23.6	14.6
	4.00	35.2			—				26.7			30.7	18.4
	5.00	43.3			36.5				35.1			37.5	22.3
	7.50	58.8			50.7				43.7			48.1	29.0
10^4[Ligand]$_0$ (M)		2.5			2.3				2.5			2.7	2.3

observed relaxation times may be represented by

$$1/\tau_{obsd} = k_{1f}([\bar{M}] + [\bar{L}]) + k_{1r} \qquad (1)$$

where k_{1f} = overall forward rate constant, k_{1r} = overall reverse rate constant, $[\bar{M}]$ = equilibrium concentration of all the metal oxyanion species, and $[\bar{L}]$ = equilibrium concentration of all the ligand species present. Since $[\bar{L}] \ll [\bar{M}]$, $[\bar{M}]$ is approximately equal to the initial concentration, $[M]_0$, of metal oxyanion, and the expression becomes,

$$1/\tau_{obsd} = k_{1f}[M]_0 + k_{1r} \qquad (2)$$

Table II. Observed Relaxation Times for the 1:1 Complexation of Tungstate with Catechol Derivatives

Ligand	$10^2[WO_4^{2-}]$ (M)	$1/\tau_{obsd}$ (s^{-1}) pH 8.00	8.20	8.50	8.85	9.00
1,2,4-Trihydroxybenzene	0.25	—	1.76	—	—	—
	0.50	1.96	2.65	1.74	1.95	0.541
	1.00	2.45	5.96	4.48	1.82	0.600
	2.50	5.86	14.6	13.1	7.50	4.35
	5.00	15.3	17.0	24.5	18.3	17.2
	7.50	25.3	—	38.1	28.5	25.9
$10^4[Ligand]_0$ (M)		2.1	2.0	2.1	2.1	2.1
Pyrogallol	0.25	—	5.23	—	—	4.35
	0.50	11.6	9.18	5.64	3.66	7.95
	1.00	21.2	15.0	7.65	8.25	17.6
	2.50	49.2	32.3	24.1	18.5	42.9
	5.00	89.7	41.3	56.9	29.0	67.1
	7.50	111.	—	65.0	60.1	—
$10^4[Ligand]_0$ (M)		1.1	1.2	0.95	1.1	0.99
Gallic acid	0.25	—	4.93	—	—	—
	0.50	6.38	9.14	9.32	9.39	9.95
	1.00	11.5	17.2	19.8	15.6	17.7
	2.50	27.1	38.0	42.8	34.4	43.1
	5.00	52.8	63.5	73.7	63.2	68.7
	7.50	78.9	—	82.7	73.5	88.7
$10^4[Ligand]_0$ (M)		1.0	1.0	0.91	1.0	1.1
Epinephrine	0.25	—	1.20	—	—	1.39
	0.50	2.32	2.33	2.70	2.58	2.27
	1.00	4.42	4.58	4.59	4.79	4.48
	2.50	9.83	9.86	10.4	10.9	10.3
	5.00	19.2	17.6	20.1	19.1	17.3
	7.50	25.9	—	27.4	26.1	—
$10^4[Ligand]_0$ (M)		0.93	0.99	1.0	0.97	1.0
L-Dopa	0.25	—	1.04	—	—	1.29
	0.50	2.00	1.91	2.37	2.38	2.46
	1.00	3.83	3.65	4.34	4.11	4.50
	2.50	8.52	7.89	9.51	9.55	10.2
	5.00	15.6	14.5	17.3	16.7	17.2
	7.50	20.9	—	22.6	22.9	—
$10^4[Ligand]_0$ (M)		1.1	1.0	1.2	1.0	0.98

Plots of $1/\tau_{obsd}$ vs. $[M]_0$ are linear in all cases (Figure 1), with the intercepts equal to k_{1r} and the slopes to k_{1f}. These values are tabulated in Tables III and IV.

Molybdate and 1,2,4-Trihydroxybenzene. Variation of the ligand concentration is complicated by several factors. When ligand is present in excess, it interferes with the absorbance of the complex. The rate of oxidation increases and also begins to interfere with rate determinations. The coupling of the first and second steps is difficult to resolve. Finally, most of the catechol derivatives are not sufficiently soluble for such studies. However, in order to demonstrate that no error is made with respect to the rate constants for the first step, and to obtain data for at least one second step complexation, the chelation of molybdate by 1,2,4-trihydroxybenzene was studied for ligand dependence as well as for molybdate dependence. Treatment of the data for this system will be explained in detail in order to establish a basis for the general treatment of oxyanion complexation with catechol derivatives.

Scheme I

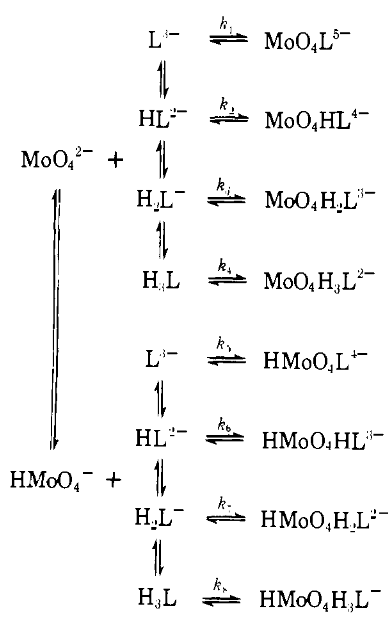

Consideration of the variously protonated forms of 1,2,4-trihydroxybenzene and molybdate leads to Scheme I for the first step.

Utilizing detailed balance, and the acid dissociation constants of molybdate and ligand, one can express the overall forward rate constant as

$$\begin{aligned} k_{1f} = {} & (k_1K_mK_{a1}K_{a2}K_{a3} + k_2K_mK_{a1}K_{a2}[H^+] \\ & + k_3K_mK_{a1}[H^+]^2 + k_4K_m[H^+]^3 + k_5[H^+]K_{a1}K_{a2}K_{a3} \\ & + k_6[H^+]^2K_{a1}K_{a2} + k_7[H^+]^3K_{a1} \\ & + k_8[H^+]^4)/(K_m + [H^+])(K_{a1}K_{a2}K_{a3} \\ & + K_{a1}K_{a2}[H^+] + K_{a1}[H^+]^2 + [H^+]^3) \end{aligned} \quad (3)$$

where $K_m = [H^+][MoO_4^{2-}]/[HMoO_4^-] \sim 10^{-4}$, $K_{a1} = [H^+][H_2L^-]/[H_3L] = 10^{-9.08}$, $K_{a2} = [H^+][HL^{2-}]/[H_2L^-] = 10^{-11.82}$, and $K_{a3} = [H^+][L^{3-}]/[HL^{2-}] \sim 10^{-13}$.

Table III. Apparent Forward and Reverse Rate Constants for the Complexation of Molybdate with Catechol Derivatives[a]

Ligand pH	1,2,4-Trihydroxybenzene	Pyrogallol	Gallic acid	Epinephrine	L-Dopa
		k_{1f} (M^{-1} s^{-1})			
7.3	814. ± 71.	1080 ± 50	3810 ± 270	682 ± 30	789 ± 52
7.7	—	2770 ± 230	3420 ± 60	697 ± 20	—
7.8	520. ± 29.	—	—	—	—
8.0	—	2730 ± 160	2810 ± 120	681 ± 37	601 ± 4
8.2	507. ± 19.	—	—	—	—
8.3	—	—	2090 ± 90	613 ± 17	—
8.4	—	2040 ± 270	—	—	—
8.5	303. ± 18.	—	—	—	544 ± 25
8.6	—	835 ± 53	—	—	—
8.7	337. ± 14.	—	—	—	—
8.8	312. ± 5.	—	—	—	618 ± 20
9.0	219. ± 17.	274 ± 35	—	—	389 ± 9
		k_{1r} (s^{-1})			
7.3	14. ± 1.	14. ± 3.	21. ± 4	6.6 ± 0.8	4.0 ± 1.2
7.7	—	20. ± 3.	18. ± 1	6.8 ± 0.4	—
7.8	19. ± 1.	—	—	—	—
8.0	—	18. ± 2.	19. ± 7	6.7 ± 0.7	6.5 ± 0.2
8.2	15. ± 0.3	—	—	—	—
8.3	—	—	14. ± 1	6.5 ± 0.3	—
8.4	—	7.6 ± 9.8	—	—	—
8.5	27. ± 1.	—	—	—	5.6 ± 0.5
8.6	—	11. ± 1.	—	—	—
8.7	8.3 ± 0.5	—	—	—	—
8.8	9.7 ± 0.2	—	—	—	4.6 ± 0.4
9.0	9.7 ± 0.5	8. ± 1.	—	—	2.7 ± 0.4

[a] No studies were carried out at a given pH where there is a blank.

Table IV. Apparent Forward and Reverse Rate Constants for the Complexation of Tungstate with Catechol Derivatives

Ligand pH	1,2,4-Trihydroxybenzene	Pyrogallol	Gallic acid	Epinephrine	L-Dopa
			k_{1f} (M^{-1} s^{-1})		
8.00	260 ± 41	1580 ± 110	1030 ± 1	372 ± 9	305 ± 14
8.20	432 ± 73	1220 ± 116	1500 ± 90	368 ± 24	299 ± 12
8.50	523 ± 10	883 ± 76	1340 ± 180	369 ± 10	313 ± 17
8.85	316 ± 65	597 ± 55	1130 ± 80	357 ± 12	309 ± 13
9.00	448 ± 60	863 ± 43	1340 ± 110	369 ± 21	373 ± 27
			k_{1r} (s^{-1})		
8.00	0.60 ± 0.34	3.9 ± 0.9	1.2 ± 0.1	0.47 ± 0.08	0.54 ± 0.16
8.20	0.62 ± 0.31	2.3 ± 0.5	1.3 ± 0.5	0.37 ± 0.12	0.32 ± 0.06
8.50	−0.87 ± 0.08	−0.86 ± 0.99	5.4 ± 2.6	0.88 ± 0.12	1.0 ± 0.3
8.85	−1.0 ± 0.08	0.83 ± 0.60	4.2 ± 1.5	1.2 ± 0.3	0.95 ± 0.22
9.00	0.19 ± 0.55	−0.47 ± 0.47	3.4 ± 1.0	0.50 ± 0.15	0.43 ± 0.14

A similar expression can be written for k_{1r}. However, because it involves the acid dissociation constants of the complexes, which are unknown, such an expression is not very useful. Apparently for similar reasons, other workers[10] have not pursued expressions for k_{1r}.

Under the conditions of this study (pH ranged from 7.3 to 9.0) $K_m \gg [H^+]$, and the terms $K_{a1}K_{a2}K_{a3}$ and $K_{a1}K_{a2}[H^+]$ are negligible with respect to $K_{a1}[H^+]^2$ and $[H^+]^3$. Thus the denominator in eq 3 becomes $K_m(K_{a1} + [H^+])[H^+]^2$, and,

$$k_{1f}(K_{a1} + [H^+]) = \frac{k_1K_{a1}K_{a2}K_{a3}}{[H^+]^2} + \frac{k_2K_{a1}K_{a2}}{[H^+]} + k_3K_{a1} + k_4[H^+] + \frac{k_5K_{a1}K_{a2}K_{a3}}{K_m[H^+]} + \frac{k_6K_{a1}K_{a2}}{K_m} + \frac{k_7K_{a1}[H^+]}{K_m} + \frac{k_8[H^+]^2}{K_m} \quad (4)$$

A plot of $k_{1f}(K_{a1} + [H^+])$ vs. $[H^+]$ is linear (Figure 2), which implies that the pathways represented by k_1, k_2, k_5, and k_8 do not contribute significantly to the overall forward rate constant. The slope of this plot equals $k_4 + k_7K_{a1}/K_m = 5.52 \times 10^2$, and the intercept is equal to $k_3K_{a1} + k_6K_{a1}K_{a2}/K_m = 1.67 \times 10^{-8}$ (see Table VIII, footnote *a*). If $k_4 \gg k_7K_{a1}/K_m$, $k_4 = 5.5 \times 10^2$ (M^{-1} s^{-1}), but if $k_7K_{a1}/K_m \gg k_4$, $k_7 = 6.6 \times 10^7$ (M^{-1} s^{-1}). If $k_3K_{a1} \gg k_6K_{a1}K_{a2}/K_m$, $k_3 = 7.9 \times 10^1$ (M^{-1} s^{-1}), and conversely, if $k_6K_{a1}K_{a2}/K_m \gg k_3K_{a1}$, $k_6 = 5.3 \times 10^9$ (M^{-1} s^{-1}). These values represent upper limits only.

The treatment of the second step

$$ML + L \underset{k_{2r}}{\overset{k_{2f}}{\rightleftharpoons}} ML_2$$

is more complicated than that of the first because the rate equations for the first and second step are coupled. The reciprocal relaxation times are the roots of the associated quadratic characteristic equation and are given by[24]

$$1/\tau_{\pm} = [(a_{11} + a_{22}) \pm \sqrt{(a_{11} + a_{22})^2 - 4(a_{11}a_{22} - a_{12}a_{21})}]/2 \quad (5)$$

where $a_{11} = k_{1f}([\bar{M}] + [\bar{L}]) + k_{1r}$, $a_{12} = k_{1r}$, $a_{21} = k_{2f}([\bar{L}] - [\overline{ML}])$, and $a_{22} = k_{2f}([\overline{ML}] + [\bar{L}]) + k_{2r}$. Under the conditions of these experiments, $[M]_{total} \ll [L]_{total}$, $[\bar{L}] \sim [L]_0$, $[\bar{M}] \ll [\bar{L}]$, and $[\overline{ML}] \ll [\bar{L}]$, so, $a_{11} \cong k_{1f}[L]_0 + k_{1r}$, $a_{12} \cong k_{1r}$, $a_{21} \cong k_{2f}[L]_0$, and $a_{22} \cong k_{2f}[L]_0 + k_{2r}$.

Values for the observed relaxation times for the complexation of molybdate and 1,2,4-trihydroxybenzene, at ionic strength 0.1 M, are given in Table V. The overall forward and reverse rate constants for the first step were calculated as outlined previously, and these values were substituted into the characteristic polynomial for which eq 5 is the solution, together with the values for $[L]_0$ and $1/\tau_{obsd}$. The values of k_{2f} and k_{2r} thus determined are also given in Table V. When the values of k_{1f}, k_{1r}, k_{2f}, and k_{2r} are substituted back into eq 5, $1/\tau_{obsd}$ is found in all cases to correspond to the negative root.

General Treatment for the First Step. Because of the various protonated forms possible for both the metal oxyanions and the ligands, a general complexation reaction scheme (Scheme II) can be written (X = Mo,W)

Scheme II

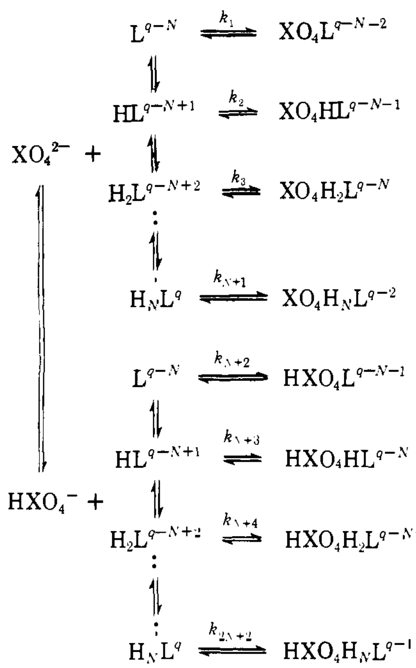

where N = number of ionizable protons of the ligand ($N = 2$ for catechol; 3 for 1,2,4-trihydroxybenzene and pyrogallol; 4 for gallic acid, L-Dopa, and epinephrine); and q equals the charge on the fully protonated ligand ($q = 0$ for catechol, 1,2,4-trihydroxybenzene, pyrogallol, and gallic acid; $q = +1$ for epinephrine and L-Dopa).

Making use of detailed balance and the various equilibrium constants, one may then write

$$k_{1f} = \frac{\sum_{i=1}^{N+1} \left\{ [H^+]^{i-1}(k_i K_m + [H^+]k_{i+N+1}) \prod_{j=0}^{N-i+1} K_{aj} \right\}}{(K_m + [H^+]) \left\{ \sum_{i=1}^{N+1} \left([H^+]^{i-1} \prod_{j=0}^{N-i+1} K_{aj} \right) \right\}} \quad (6)$$

where $K_{a0} \equiv 1$, $K_{a1} \equiv [H^+][H_{N-1}L^{q-1}]/[H_N L^q]$, and $K_{ai} \equiv [H^+][H_{N-i}L^{q-i}]/[H_{N-i+1}L^{q-i+1}]$.

Specific values of K_{ai} for given ligands and oxyanions (Table VI), allow the denominators in eq 6 to be simplified by eliminating terms which do not contribute significantly. The equation can then be rearranged slightly and written in the general form,

$$k_{1f}Q = R/S \quad (7)$$

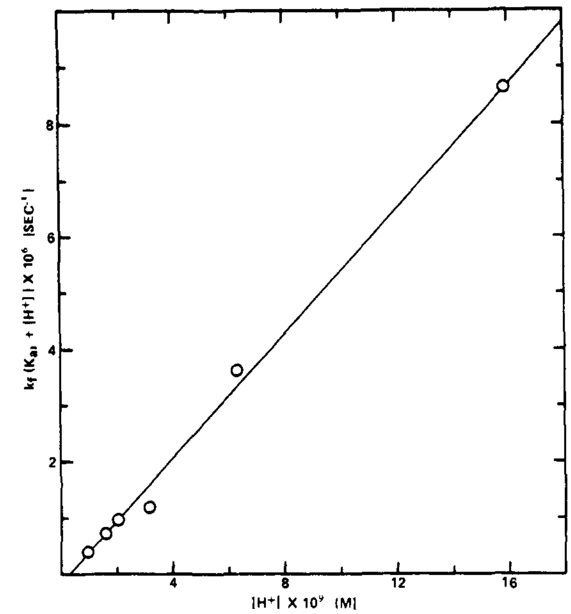

Figure 2. Plot of $k_{1f}(K_{a1} + [H^+])$ against $[H^+]$ for molybdate plus 1,2,4-trihydroxybenzene, 1:1 step (T = 25 °C, ionic strength = 0.5 M). Calculated least-squares straight lines have been drawn through the data points.

Table V. Molybdate Plus 1,2,4-Trihydroxybenzene Relaxation Times and Rate Constants

First Step: Molybdate in Excess, M + L ⇄ ML; $[L]_0 = 2.1 \times 10^{-4}$ M.

$10^2[MoO_4^{2-}]$ (M)	$1/\tau_{obsd}$ (s^{-1}) pH 7.0	7.3	7.8
3.02	—	31.6	—
2.02	—	24.3	—
1.51	20.4	15.8	15.3
1.01	16.6	14.8	13.6
0.76	13.6	14.0	11.8
0.50	11.3	11.1	10.8
0.37	10.2	—	9.56
0.20	—	7.97	—
k_{1f} ($M^{-1} s^{-1}$)	913. ± 39.	831. ± 29.	497. ± 48.
k_{1r} (s^{-1})	6.8 ± 0.4	6.9 ± 0.5	8.1 ± 0.4

Two Coupled Steps: Ligand in Excess, M + 2L ⇄ ML + L ⇄ ML_2; $[M]_0 = 3.0 \times 10^{-5}$ M.

10^2[1,2,4-Trihydroxybenzene] (M)	$1/\tau_{obsd} = 1/\tau_-$ (s^{-1}) pH 7.0	7.3	7.7
1.52	—	1.61	—
1.40	—	—	2.29
1.27	.72	—	—
1.17	—	—	2.09
1.02	.71	—	—
.97	—	.88	—
.64	.61	—	1.39
.61	—	.72	—
.51	—	—	1.18
.49	—	.60	—
.33	.44	—	—
.31	—	—	.87
.29	—	.46	—
k_{2f} ($M^{-1} s^{-1}$)	29.3 ± 6.7	131. ± 11.	269. ± 57.
k_{2r} (s^{-1})	0.38 ± 0.07	0.35 ± 0.07	1.0 ± 0.2

Table VI. pK_a's Used in This Paper

Reactant	pK_{a1}	pK_{a2}	pK_{a3}	pK_{a4}	Ref
Molybdate	~4	4			a
Tungstate	3.5	2.3			b
1,2,4-Trihydroxybenzene	9.08	11.82	>13		c
Pyrogallol	9.28	11.43	~14		c
Gallic acid	4.22	8.38	10.49	13.1	d, e
Epinephrine	2.58	8.7	10.0	~13	f, g
L-Dopa	2.3	8.8	9.8	13.0	g, h

[a] L. G. Sillen and A. E. Martell, *Chem. Soc., Spec. Publ.*, **No. 25**, 41 (1971). Cf. J. J. Cruywagen and E. F. C. H. Rohwer, *Inorg. Chem.*, **14**, 3136 (1975). [b] L. G. Sillen and A. E. Martell, *Chem. Soc., Spec. Publ.*, **No. 25**, 45 (1971). [c] J. Sunkel and H. Staude, *Ber. Bunsenges. Phys. Chem.*, **72**, 567 (1968). [d] G. Ackermann, D. Hesse, and P. Volland, *Z. Anorg. Allg. Chem.*, **377** (1), 92 (1970). [e] K. Gilbert, unpublished results. [f] A. C. Andrews, T. D. Lyons, and T. D. O'Brien, *J. Chem. Soc.*, 1776 (1962). [g] R. B. Martin, *J. Phys. Chem.*, **75**, 2657 (1971). [h] J. E. Gordon and R. F. Jameson, *J. Chem. Soc. A*, 2615 (1968).

where

$$R = \sum_{i=1}^{N+1} \left\{ [\mathrm{H}^+]^{i-1}(k_i K_m + [\mathrm{H}^+]k_{i+N+1}) \prod_{j=0}^{N-i+1} K_j \right\}$$

and the expressions for Q and S are tabulated in Table VII for specific oxyanion-ligand systems. Plots of $k_{1f}Q$ vs. $[\mathrm{H}^+]$ for the ten systems studied give straight lines with slopes and intercepts as given in Table VIII. Therefore, for both molybdate and tungstate, the only pathways which contribute to the overall forward rate in Scheme II are 3, 4, 6 and 7 for 1,2,4-trihydroxybenzoic acid and pyrogallol, and pathways 3, 4, 7, and 8 for gallic acid, epinephrine, and L-Dopa.

The slope is equal to the sum of two terms, one a function of k_{N+1} (or k_N, for gallic acid, epinephrine, or L-Dopa) and the other of k_{2N+1} (or k_{2N}). These terms are not distinguishable kinetically, as the pathways they represent are related by a proton transfer from ligand to metal oxyanion; these are the "acid dependent" terms. Similarly, the intercept is the sum of a term depending on k_N (or k_{N-1}, for gallic acid, epinephrine, or L-Dopa) and another term depending on k_{2N} (or k_{2N-1}). These rate constants are also related by a proton transfer from ligand to metal oxyanion and are kinetically indistinguishable; these are the "acid-independent" terms. For those intercepts which were negative, the maximum value was taken to be the intercept plus three times the standard deviation.

Upper limits for the values of the individual rate constants can be found by setting one term equal to zero in each of these coupled expressions and solving for the remaining rate constants, as in the molybdate-1,2,4-trihydroxybenzene example. In this way maximum values are found for all four pathways allowed for each system. These values are tabulated in Table IX.

Some of the values for upper limits exceed diffusion-controlled rate constants; e.g., in the third column of Table IX, k_{2N} or k_{2N-1}, for the complexation of HXO_4^- with $H_{N-2}L$, or $H_{N-3}L$ (doubly or triply charged). If we set the diffusion-controlled rate constant for these reactions at 1.0×10^9 M^{-1} s^{-1}, we can use this value toobtain a *minimum* value for k_N or k_{N-1}, with which these reactions are coupled kinetically. The minimum values of k_N, or k_{N-1}, as determined, are given in Table X together with the maximum values previously determined.

Discussion

For the ligand-oxyanion systems studied, there is no significant contribution to the reaction rate from pathways which apparently can have no proton transfer, for example, from a pathway of a completely deprotonated ligand, L^{q-N}, reacting with MoO_4^{2-}, or a completely protonated ligand, H_NL^q, reacting with $HMoO_4^-$. Furthermore, since some of the values for the kinetically indistinguishable pathways exceed diffusion control, minimum values were established for the reaction $XO_4^{2-} + H_{N-1}L$ (or $H_{N-2}L$) (X = Mo or W). The upper and lower limits for the rate constants of these pathways are approximately the same, within the uncertainty in the pK_a's of the ligands and oxyanions, and the arbitrariness of choosing a value for the diffusion-limited rate constant. Therefore, the unprotonated forms of molybdate and tungstate contribute to the overall forward reaction rate, and the values given in columns three and four of Table X for k_{N-1} (or k_{N-2}) are approximately the actual values, and not merely limits.

To examine the trends in basicity, consider Tables XI and XII where the ligands are arranged vertically in the order of increasing rate constant. Also included in Tables XI and XII are rate constants from other studies[9-13] for the complexation of molybdate and tungstate with additional ligands. Some of these ligands are not catechol derivatives and contain chelating nitrogen atoms. The pK_a's are also listed, and the ligands are grouped according to reaction with XO_4^{2-} or HXO_4^-.

Reading across the table shows an increase in rate constants. Thus, the protonated oxyanion is generally more reactive than the unprotonated, as has been noted.[10] However, comparing protonated with unprotonated oxyanion and reading down the table shows that, if the oxyanion is protonated, it is the most basic ligand that is most reactive. If the oxyanion is not protonated, the least basic ligand is more reactive.

To understand these trends we begin with a consideration of the structures of the oxyanions in solution. The structure is tetrahedral in the crystalline state of the uncomplexed oxyanions such as sodium molybdate and sodium tungstate,[25-29]

Table VII. Specific Q and S Expressions

$$k_{1f}Q = \frac{R}{S} \quad R = K_m \sum_{i=1}^{N+1} \left([\mathrm{H}^+]^{i-1} k_i \prod_{j=0}^{N-i+1} K_{aj} \right) + \sum_{i=1}^{N+1} \left(k_{i+N+1} [\mathrm{H}^+]^i \prod_{j=0}^{N+1-i} K_{aj} \right)$$

Ligand	Q	S
Catechol	$K_{a1} + [\mathrm{H}^+]$	$K_m[\mathrm{H}^+]$
1,2,4-Trihydroxybenzene	$K_{a1} + [\mathrm{H}^+]$	$K_m[\mathrm{H}^+]^2$
Pyrogallol	$K_{a1} + [\mathrm{H}^+]$	$K_m[\mathrm{H}^+]^2$
Gallic acid	$K_{a2} + [\mathrm{H}^+] + \frac{K_{a2}K_{a3}}{[\mathrm{H}^+]}$	$K_m[\mathrm{H}^+]^2K_{a1}$
Epinephrine	$K_{a2} + [\mathrm{H}^+] + \frac{K_{a2}K_{a3}}{[\mathrm{H}^+]}$	$K_m[\mathrm{H}^+]^2K_{a1}$
L-Dopa	$K_{a2} + [\mathrm{H}^+] + \frac{K_{a2}K_{a3}}{[\mathrm{H}^+]}$	$K_m[\mathrm{H}^+]^2K_{a1}$

Table VIII. Slopes and Intercepts from Plots of $k_{1f}Q$ vs. $[H^+]$

Ligand	Expression for: Slope	Intercept
Catechol	$k_3 + k_5\frac{K_{a1}}{K_m}$	$k_2K_{a1} + k_4\frac{K_{a1}K_{a2}}{K_m}$
1,2,4-Tihydroxybenzene	$k_4 + k_7\frac{K_{a1}}{K_m}$	$k_3K_{a1} + k_6\frac{K_{a1}K_{a2}}{K_m}$
Pyrogallol	$k_4 + k_7\frac{K_{a1}}{K_m}$	$k_3K_{a1} + k_6\frac{K_{a1}K_{a2}}{K_m}$
Gallic acid	$k_4 + k_8\frac{K_{a2}}{K_m}$	$k_3K_{a1} + k_7\frac{K_{a2}K_{a3}}{K_m}$
Epinephrine	$k_4 + k_8\frac{K_{a2}}{K_m}$	$k_3K_{a2} + k_7\frac{K_{a2}K_{a3}}{K_m}$
L-Dopa	$k_4 + k_8\frac{K_{a2}}{K_m}$	$k_3K_{a2} + k_7\frac{K_{a2}K_{a3}}{K_m}$

Ligand	Values for: Slope (M^{-1} s^{-1}) Mo	W	Intercept (s^{-1}) Mo	W
Catechol[b]	3.0×10^2	1.09×10^2	1.9×10^{-7}	8.09×10^{-8}
1,2,4-Trihydroxybenzene	$5.52(\pm0.58) \times 10^2$		$-1.36(\pm1.01) \times 10^{-8}$ [a]	
Pyrogallol	$1.10(\pm0.04) \times 10^3$	$1.25(\pm0.31) \times 10^3$	$-6.14(\pm3.41) \times 10^{-7}$ [a]	$-1.48(\pm4.41) \times 10^{-7}$ [a]
Gallic acid	$4.25(\pm0.02) \times 10^3$	$8.64(\pm1.20) \times 10^2$	$-2.39(\pm0.24) \times 10^{-6}$ [a]	$5.96(\pm1.20) \times 10^{-6}$
Epinephrine	$7.17(\pm0.20) \times 10^2$	$3.69(\pm0.06) \times 10^2$	$7.56(\pm1.69) \times 10^{-7}$	$7.64(\pm0.19) \times 10^{-7}$
L-Dopa	$6.47(\pm0.30) \times 10^2$	$3.52(\pm0.51) \times 10^2$	$5.35(\pm1.45) \times 10^{-7}$	$5.31(\pm1.57) \times 10^{-7}$

[a] For negative intercepts, the expression was set equal to the intercept + 3 times the standard deviation. [b] Calculated using data from ref 11 and 13.

but the aqueous state is less well defined. Although there is some evidence that an octahedral form exists in solution,[12,30] its presence has been most closely associated with the protonated oxyanion.[15,17,30] Addition of a proton is then thought to involve coordination of two water molecules leading to an octahedral complex as $Mo(O)_2(OH)_3H_2O^-$ [30] or $MoO(OH)_5^-$.[31] The structure $Mo(O)_2(OH)_3H_2O^-$ has been inferred from ^{95}Mo and ^{97}Mo NMR studies on aquo molybdate.[30] Thus, at least one structural form of protonated, unchelated oxyanion would be related in coordination number and electronic structure to the octahedrally coordinated chelates, which are well defined both in solid state and solution.[16]

If the protonated oxyanion is octahedral, then complex formation of, for example, molybdate with a catechol derivative will be by a substitution reaction, and two of molybdenum's oxygen groups will have to leave. Since at least one of these groups is hydroxide ion, which is presumably tightly bound, it is difficult to reconcile such a rapid, facile substitution with such a poor leaving group.[32] However, the departure of the metal-bound oxygen will be aided if, instead of hydroxide ion, a water molecule is removed from the central metal atom, while a hydroxide ion is inserted into the solution at a point more remote from the oxyanion. This changeover can be achieved through hydrogen bond assisted proton transfer. A more basic ligand binding site orients water molecules more favorably about the leaving OH^- group and thereby assists in the process. This mechanism is illustrated below for doubly deprotonated catechol reacting with protonated molybdate in the cis-dioxo form suggested in the NMR study.[30]

stoichiometry: $Mo(O)_2(OH)_3H_2O^- + C_6H_4O_2^{2-}$

$$\rightleftharpoons Mo(O)_2(OH)_2C_6H_4O_2^{2-} + H_2O + OH^-$$

mechanism:

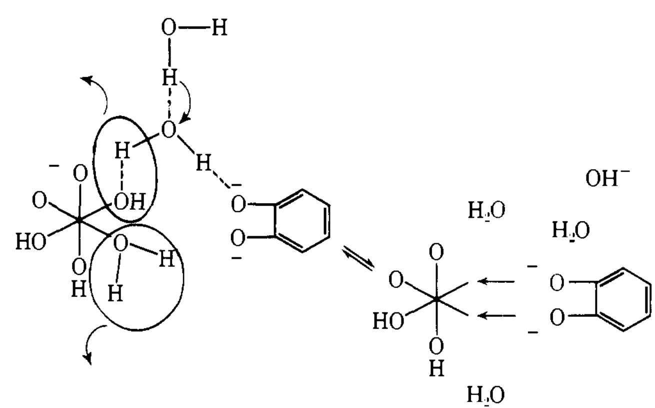

Therefore, the rate of complex formation of protonated molybdate with doubly deprotonated ligand oxygen binding sites increases with increasing basicity (columns five and eight, Tables XI, XII). If the structure of the protonated molybdate is $MoO(OH)_5^-$ rather than $Mo(O)_2(OH)_3H_2O^-$, the mechanism for reaction with doubly deprotonated catechol would be similar to that given above, except that both leaving groups would be hydroxy ions, and both would be assisted by such a proton transfer.

Suppose, now, that one of the ligand's complexing oxygen atoms is protonated and one is not. The unprotonated, hydrogen-bonding oxygen must be correctly oriented with respect to the hydroxy, rather than the water, of the metal-containing oxyanion; then, the hydroxy group can be assisted by proton transfer in leaving as a water molecule. This steric requirement would be expected to reduce the rate of complexation. In addition, the protonated ligand binding site will be less nucleophilic for the oxyanion's central metal atom, and this effect might influence ring closure. Hence, with respect to full deprotonation of the ligand chelating atoms, a ligand with one

Table IX. Upper Limits for Individual Forward Rate Constants ($M^{-1}\ s^{-1}$)

	MoO_4^{2-} +		$HMoO_4^-$ +	
Ligand	$H_{N-1}L$ k_N	H_NL k_{N+1}	$H_{N-2}L$ k_{2N}	$H_{N-1}L$ k_{2N+1}
Catechol[a]	3.0×10^2	3.0×10^2	3.0×10^{10}	4.8×10^7
1,2,4-Trihydroxybenzene	7.9×10^1	5.5×10^2	5.3×10^9	6.6×10^7
Pyrogallol	1.3×10^2	1.1×10^3	3.6×10^9	2.1×10^8
Oxine-SO_3^- [b]	2.5×10^3	5.0×10^6	$\sim 4.0 \times 10^7$	$\sim 3.9 \times 10^6$
Oxine[c]	4.1×10^2	5.0×10^5	$\sim 1.5 \times 10^8$	$\sim 4.5 \times 10^6$
	$H_{N-2}L$ k_{N-1}	$H_{N-1}L$ k_N	$H_{N-3}L$ k_{2N-1}	$H_{N-2}L$ k_{2N}
Epinephrine	3.8×10^2	7.2×10^2	3.8×10^8	3.6×10^7
L-Dopa	3.3×10^2	6.5×10^2	2.1×10^8	4.0×10^7
Gallic acid		4.25×10^3		1.0×10^8
	WO_4^{2-} +		HWO_4^- +	
	$H_{N-1}L$ k_N	H_NL k_{N+1}	$H_{N-2}L$ k_{2N}	$H_{N-1}L$ k_{2N+1}
Catechol[d]	1.3×10^2	1.1×10^2	1.3×10^{10}	1.7×10^7
Pyrogallol	5.6×10^2	1.3×10^3	4.7×10^{10}	7.5×10^8
Oxine-SO_3^- [b]	1.3×10^4	$<1.5 \times 10^6$	$\sim 6.2 \times 10^8$	$<3 \times 10^6$
Oxine[b]	2.4×10^3	2.0×10^5	$\sim 2.6 \times 10^9$	$\sim 5.4 \times 10^6$
	$H_{N-2}L$ k_{N-1}	$H_{N-1}L$ k_N	$H_{N-3}L$ k_{2N-1}	$H_{N-2}L$ k_{2N}
Epinephrine	3.8×10^2	3.7×10^2	1.2×10^9	5.8×10^7
L-Dopa	3.3×10^2	3.5×10^2	6.6×10^8	7.0×10^7
Gallic acid	1.4×10^3	8.6×10^2	1.4×10^{10}	6.6×10^7

[a] Calculated from data in ref 11. [b] From ref 10. [c] From ref 9. [d] Calculated from data in ref 13.

Table X. Upper and Lower Limits for Rate Constants ($M^{-1}\ s^{-1}$)

		Molybdate		Tungstate	
Ligand	k_i	Lower limit	Upper limit	Lower limit	Upper limit
Catechol[a]	k_2	2.9×10^2	3.0×10^2	1.2×10^2	1.3×10^2
1,2,4-Trihydroxybenzene	k_3	6.4×10^1	7.9×10^1		
Pyrogallol	k_3	0.95×10^2	1.3×10^2	5.5×10^2	5.6×10^2
Gallic acid	k_3			1.3×10^3	1.4×10^3
Epinephrine	k_3			6.6×10^1	3.8×10^2

[a] Calculated using data from ref 11 and 13.

chelating atom protonated would be expected to react more slowly. Columns five and eight of Tables XI and XII show that this effect is consistently observed for each ligand by at least one order of magnitude. Even though the overall complexation rate constant has been depressed relative to full deprotonation, the rate constants for the different ligands are still seen to increase with increasing basicity.

This same form of ligand—one chelating oxygen protonated and one not—reacts more slowly (about three to six orders of magnitude) with unprotonated oxyanion than it does with protonated oxyanion. Moreover, the dependence of the rate constant on pK_a is exactly opposite. The rate of complexation of singly protonated ligand with unprotonated oxyanion *decreases* with increasing basicity. These two observations strongly suggest that the oxyanion species is fundamentally different in the protonated and deprotonated forms. If, for example, unprotonated oxyanion exists tetrahedrally coordinated and protonated oxyanion octahedrally coordinated with one or two water molecules present, complexation of unprotonated oxyanion would be an addition, rather than a substitution reaction, and would be likely to show differences in rates and dependencies from complexation of protonated oxyanion. Furthermore, since no oxygen-containing group such as OH^- or H_2O leaves the unprotonated oxyanion, oriented water molecules are of no help and, in fact, may hinder complexation. The rate of complex formation would then increase with decreasing basicity.

This explanation can be tested on a trend in higher order substitution which differs from that observed in the formation of the mono complex. That is, whereas for the first step the overall forward rate of complexation decreases with increasing pH, that of the second step increases. Protonated oxyanion reacts faster than unprotonated oxyanion, regardless of the ligand form, and the more deprotonated ligand reacts faster with protonated oxyanion. The degree of protonation of the oxyanion is seen to have the more powerful effect on the rate of complexation than the degree of protonation of the ligand. (Compare the rate constants of column 2 with column 5 in Table IX, in contrast with the rate constants of column 4 vs. column 5.) This effect may be due to the postulated difference in structure of the oxyanions—tetrahedral if unprotonated and octahedral if protonated. Thus, for the first step (1:1 complexation) the *overall* forward reaction will be faster as more protonated oxyanion exists, i.e., at lower pH's. For the second step, the metal-containing reactant is already in octahedral coordination, and the degree of protonation of the ligand as-

Table XI. Effect of Basicity of Ligand on Reactivity with Molybdate

Form of molybdate: Form of ligand:[a] Ligand[b]	MoO_4^{2-} + A BH k (M^{-1} s^{-1})	pK_a	Ligand	$HMoO_4^-$ + A BH k (M^{-1} s^{-1})	pK_a	Ligand[b]	$HMoO_4^-$ + A B k (M^{-1} s^{-1})	pK_a
1,2,4-Trihydroxybenzene	0.76×10^2	9.1	EDTA[g]	2.26×10^5	2.0	EDTA[g]	2.26×10^5	2.0
Pyrogallol	1.3×10^2	9.3	Oxine-SO_3^- [e]	$\sim 3.9 \times 10^6$	3.9	Oxine-SO_3^- [e]	4.0×10^7	8.2
Catechol[c]	3.0×10^2	9.2	Oxine[d,f]	4.5×10^6	5.0	Oxine[d,f]	1.5×10^8	9.6
L-Dopa	3.3×10^2	8.8	Epinephrine	3.6×10^7	8.7	L-Dopa	2.1×10^8	9.8[h]
Epinephrine	3.8×10^2	8.7	L-Dopa	4.0×10^7	8.8	Epinephrine	3.8×10^8	10.0[h]
Oxine[d,f]	4.1×10^2	5.0	Catechol[c]	4.8×10^7	9.2	Pyrogallol	3.6×10^9	11.4
Oxine-SO_3^- [e]	2.5×10^3	3.9	1,2,4-Trihydroxybenzene	6.6×10^7	9.1	1,2,4-Trihydroxybenzene	5.3×10^9	11.8
			Gallic acid[f]	1.0×10^8	8.4	Catechol[c]	3.0×10^{10}	12.0
			Pyrogallol	2.1×10^8	9.3			

[a] A and B represent the unprotonated atoms. For catechol and its derivatives, A = B = oxygen; for oxine and oxine-SO_3^-, A = nitrogen, B = oxygen; see footnote *g* regarding EDTA. The pK_a's given represent those for AH in the first two (identical) ligand forms and those for BH in the third ligand form. [b] No values were obtainable for gallic acid due to its negative intercept (Table VIII). [c] Values calculated using data from ref 11. [d] From ref 9. [e] From ref 10. [f] The rate constants for oxine should be "normalized" to account for the decreased repulsion of its less negative charge. This correction would decrease the substitution rate constant relative to oxine sulfonate. Likewise, the rate constants for gallic acid should be "normalized" to account for the extra repulsion of the additional negative charge, which would increase the substitution rate constants relative to other catechol derivatives. [g] From ref 12 note that EDTA is tridentate here, with two chelating oxygens and one chelating nitrogen; since one of these is protonated, EDTA may be seen as A BH or as A B, depending on which two ligands one treats. However, as can be seen here, the rate constants fit into the trends with respect to basicity for either series. [h] Although the pK_{a3}'s for L-Dopa and epinephrine are usually not assigned to the second phenolic group, the kinetics data would seem to warrant such an assignment. The rate constants in columns 5 and 8 of Tables XI and XII differ by an order of magnitude, and so indicate a difference in the attacking site.

Table XII. Effect of Basicity of Ligand on Reactivity with Tungstate

Form of tungstate: Form of ligand:[a] Ligand	WO_4^{2-} + A BH k (M^{-1} s^{-1})	pK_a	Ligand	HWO_4^- + A BH k (M^{-1} s^{-1})	pK_a	Ligand	HWO_4^- + A B k (M^{-1} s^{-1})	pK_a
Catechol[b]	1.2×10^2	9.2	Oxine-SO_3^- [d]	$<3 \times 10^6$	3.9	Oxine-SO_3^- [d]	$\sim 6.2 \times 10^8$	8.2
3,4-Dihydroxybenzoic acid[b,c]	2.4×10^2	8.8	Oxine[c,d]	$\sim 5.4 \times 10^6$	5.0	L-Dopa	6.6×10^8	9.8[e]
L-Dopa	3.3×10^2	8.8	Catechol[b]	1.7×10^7	9.2	Epinephrine	1.2×10^9	10.0[e]
Epinephrine	3.8×10^2	8.7	3,4-Dihydroxybenzoic acid[b,c]	4.8×10^7	8.8	Oxine[c,d]	$\sim 2.6 \times 10^9$	9.6
Pyrogallol	5.6×10^2	9.3	Epinephrine	5.8×10^7	8.7	Catechol[b]	1.3×10^{10}	12.0
Gallic acid[c]	1.4×10^3	8.4	Gallic acid[c]	6.6×10^7	8.4	Gallic acid[c]	1.4×10^{10}	10.5
Oxine[c,d]	2.4×10^3	5.0	L-Dopa	7.0×10^7	8.8	Pyrogallol	4.7×10^{10}	11.4
Oxine-SO_3^- [d]	1.3×10^4	3.9	Pyrogallol	7.5×10^8	9.3	3,4-Dihydroxybenzoic acid[b,c]	7.7×10^{10}	12.0

[a] See footnote *a*, Table XI. [b] Values calculated using data from ref 13. [c] See footnote *f*, Table XI. [d] From ref 10. [e] See footnote *h*, Table XI.

sumes more importance. Consequently, the rate increases with increasing pH.

We now return to the initial observation of this section, the relative inactivity of unprotonatedolybdate with completely unprotonated ligand, and of protonated molybdate with fully protonated ligand. In line with the previous discussion, protonated molybdate requires some assistance, in the form of proton transfer from water, in the leaving of an oxygen. However, if the ligand is fully protonated, it is not as capable of orienting water molecules to assist in the proton transfer to molybdate's oxygen. Thus there is no significant contribution to the forward reaction rate from the pathway involving HXO_4^- and fully protonated ligands.

On the other hand, increased hydrogen bonding was postulated to interfere with simple addition. Thus, the reaction of tetrahedral, unprotonated oxyanion with a ligand having both chelating atoms deprotonated, which is therefore capable of maximum hydrogen bonding, does not contribute significantly to the overall forward reaction rate.

Further support for the ideas outlined in this section comes from an examination of the reaction of molybdate with molybdate. Here, one may regard one molybdate molecule as a ligand and the other as the oxyanion. The observation that unprotonated molybdate does not react with fully deprotonated ligand then correlates with the fact that molybdate is completely monomeric in basic solutions, where molybdate exists solely as the unprotonated tetrahedral ion. In slightly acidic solutions, where $HMoO_4^-$ does exist, reaction, i.e., polymerization, occurs.

Although the observed reactivity patterns suggest the interpretation advanced here, namely, that HXO_4^- is structurally different from XO_4^{2-}, the results are also compatible with ligand addition to tetrahedral HXO_4^-. Protonation of XO_4^{2-} would lengthen the metal-oxygen bond, thereby lowering the activation energy required to form the increased coordination number activated complex of an associative mechanism. The greater reactivity of the more basic ligands would then be due to the stronger bonding of these more nucleophilic ligands. Finally, the inverse trend in the reactivity of unprotonated MoO_4^{2-} and WO_4^{2-} may be illusory, as the rate constants in column two of Tables XI and XII are mainly upper limits, and the real trend, if any, may not have been demonstrated. Nevertheless, when considering the kinetics data for mono complex formation with different ligands, higher order complex formation, and the kinetics of oxyanion protonation and polymerization, the most consistently applicable mechanism seems to be associative addition to tetrahedral XO_4^{2-} and associative substitution on octahedral HXO_4^-.

Acknowledgment. The authors would like to acknowledge stimulating and clarifying discussions with Dr. H. Diebler and Drs. Regitze and Robert Vold.

References and Notes

(1) The authors gratefully acknowledge support from the Institute of General Medical Sciences, Public Health Service (Grant GM08893-12), and from the National Science Foundation (Grant GB-33617). This work is taken, in part, from the Ph.D. dissertation of K. Gilbert, Brandeis University, 1976.
(2) R. Puschel and E. Lassner, "Chelates in Analytical Chemistry", Vol. I, H. A. Flaschka and A. J. Barnard, Jr., Ed., Marcel Dekker, New York, N.Y., 1967, p 267.
(3) F. A. Cotton and G. Wilkinson, "Advanced Inorganic Chemistry", 3d ed, Interscience, New York, N.Y., 1972, p 656f.
(4) K. Kustin and J. Swinehart, *Prog. Inorg. Chem.*, **13**, 107 (1970).
(5) K. A. Muirhead, G. P. Haight, Jr., and J. K. Beattie, *J. Am. Chem. Soc.*, **94**, 3006 (1972).
(6) C.-t. Lin and J. K. Beattie, *J. Am. Chem. Soc.*, **94**, 3011 (1972).
(7) A. Haim, *Inorg. Chem.*, **11**, 3147 (1972).
(8) K. Kustin and D. L. Toppen, *J. Am. Chem. Soc.*, **95**, 3564 (1973).
(9) P. F. Knowles and H. Diebler, *Trans. Faraday Soc.*, **84**, 977 (1968).
(10) H. Diebler and R. E. Timms, *J. Chem. Soc. A*, 273 (1971).
(11) K. Kustin and S.-T. Liu, *J. Am. Chem. Soc.*, **95**, 2487 (1973).
(12) D. S. Honig and K. Kustin, *J. Am. Chem. Soc.*, **95**, 5525 (1973).
(13) S.-T. Liu and K. Kustin, *Inorg. Chem.*, **12**, 2362 (1973).
(14) R. H. Busey and O. L. Keller, Jr., *J. Chem. Phys.*, **41**, 215 (1964).
(15) D. S. Honig and K. Kustin, *J. Phys. Chem.*, **76**, 1575 (1972).
(16) Reference 3, p 967. Also, an NMR study of 8-hydroxyquinoline complexes of Mo(VI), V, and V(V) shows octahedral coordination with cis-dioxo bonding, L. W. Amos and D. T. Sawyer, *Inorg. Chem.*, **13**, 78 (1974).
(17) C. Schwarzenbach and J. Muir, *J. Inorg. Nucl. Chem.*, **8**, 302 (1958).
(18) J. Halmekoski, *Ann. Acad. Sci. Fenn., Ser. A2*, **96**, 1 (1959).
(19) L. Fernandes, *Gazz. Chim. Ital.*, **55**, 424 (1925); **56**, 416 (1926); **57**, 567 (1927).
(20) J. Halmekoski, *Suom. Kemistil. B*, **35**, 238 (1962); 241 (1962).
(21) H. R. Mahler and E. H. Cordes, "Biological Chemistry", Harper and Row, New York, N.Y., 1966, p 14.
(22) K. Kustin, S.-T. Liu, C. Nicolini, and D. L. Toppen, *J. Am. Chem. Soc.*, **96**, 7410 (1974).
(23) R. H. Moore and R. K. Zeigler, "The Solution of the General Least Squares Problem with Special Reference to High Speed Computers", Report LA-2367. Los Alamos Scientific Laboratory, Los Alamos, N.M. Available from National Technical Information Service, Springfield, Va. We wish to thank Professor David L. Toppen for modifying this program for use on the PDP-10.
(24) G. G. Hammes in "Techniques of Chemistry", Vol. VI, Part II, 3d ed, G. G. Hammes Ed., Wiley-Interscience, New York, N.Y., 1974, p 147.
(25) F. X. N. M. Kools, A. S. Koster, and G. D. Rieck, *Acta Crystallogr., Sect. B*, **26**, 1974 (1970).
(26) B. M. Gatehouse and P. Leverett, *J. Chem. Soc. A*, 849 (1969).
(27) G. M. Clark and W. P. Doyle, *Spectrochim. Acta*, **22**, 1441 (1966).
(28) I. Lindqvist, *Acta Chem. Scand.*, **4**, 1066 (1950).
(29) L. G. Sillen and A.-L. Nylander, *Ark. Kemi, Min. Geol.*, **17A** (4), 1 (1943).
(30) R. R. Vold and R. L. Vold, *J. Magn. Reson.*, **19**, 365 (1975).
(31) M. L. Freedman, *J. Am. Chem. Soc.*, **80**, 2072 (1958).
(32) F. Basolo and R. G. Pearson, "Mechanisms of Inorganic Reactions", 2d ed, Wiley, New York, N.Y., 1967, p 165.

Intramolecular Electron Transfer Mediated by 4,4′-Bipyridine and Related Bridging Groups

H. Fischer, G. M. Tom, and H. Taube*

Contribution from the Department of Chemistry, Stanford University, Stanford, California 94305. *Received February 4, 1976*

Abstract: At 25°, the first-order specific rates for the reduction of Co(III) by Ru(II) in the complexes of the type $[(NH_3)_5Co^{III}L\cdots LRu^{II}(NH_3)_4H_2O]$ with L···L as 4,4′-bipyridine, 1,2-bis(4-pyridyl)ethylene, 3,3′-dimethyl-4,4′-bipyridine, bis(4-pyridyl) sulfide, and 1,2-bis(4-pyridyl)ethane are 44×10^{-3}, 18.7×10^{-3}, 5.5×10^{-3}, 4.9×10^{-3}, and $1.20 \times 10^{-3}\ s^{-1}$, respectively. The extinction coefficients for the mixed valence species, $[(NH_3(_5Ru^{III}L\cdots LRu^{II}(NH_3)_5]$, with the same bridging ligands decrease in the same order as do the specific rates recorded, and a relation of at least limited validity between these two kinds of measurements is thereby indicated. For the Co(III)–Ru(II) complexes with the first four bridging ligands the values of $\Delta H^{\neq}$ for intramolecular electron transfer are within experimental error constant ($\Delta H^{\neq}$ ranges from 20.0 to 20.3 kcal mol^{-1}) and the small differences in rate are reflected mainly in $\Delta S^{\neq}$ which ranges from 2.6 cal $deg^{-1}\ mol^{-1}$ for the fastest reaction to −1.9 for the slowest. These results suggest that the Franck–Condon barrier for electron transfer is constant for the series, and that the slight rate differences result from the slower reactions being not quite adiabatic. In the four systems referred to, the bridging group apparently mediates in electron transfer, but in the reaction with the last-mentioned bridging ligand, electron transfer appears to take place directly between the metal centers.

Isied and Taube[1] have described a strategy for preparing complexes which contain within a single molecule Co(III) as an oxidizing agent and Ru(II) as a reducing agent, making it possible for these systems to measure the rates of net intramolecular electron transfer. Some of the advantages of such measurements over those of intermolecular rates for the purpose of understanding fundamental aspects of the charge transfer process itself have long been recognized.[1,2]

Our work is an extension of that of Isied et al.[1] We have selected for study a series in which the interaction between the metal centers can be altered while retaining about each a constant environment. The series we chose is based on 4,4′-bipyridine as the bridging group, with the changes in structure and composition being limited to the bridging group and, within it, to the connection between the pyridine rings. The study by Harriman and Maki[3] on intramolecular electron transfer in the radical anions derived from 4,4′-dinitrobiphenyl species with similar structural alterations in the 1,1′ positions